Acta Crystallographica Section D
Biological Crystallography
ISSN 0907-4449

Crystallization and preliminary X-ray analysis of the auxin receptor ABP1

Eui-Jeon Woo,[a] James Bauly,[b] Jin-Gui Chen,[b] Jacqueline Marshall,[b] Heather Macdonald,[c,d] Colin Lazarus,[c] Peter Goodenough,[e] Michael Venis,[b] Richard Napier[b] and Richard Pickersgill[a]*

[a]Queen Mary and Westfield College, Molecular and Cellular Biology, University of London, Mile End Road, London E1 4NS, England, [b]Horticulture Research International, Wellesbourne, Warwick CV35 9EF, England, [c]School of Biological Sciences, University of Bristol, Woodland Road, Bristol BS8 1UG, England, [d]Biological and Biomedical Sciences, University of the West of England, Bristol BS16 1QY, England, and [e]Department of Botany, School of Plant Sciences, The University of Reading, Reading RG6 6AS, England

Correspondence e-mail: r.w.pickersgill@qmw.ac.uk

Received 3 April 2000
Accepted 31 July 2000

Auxin-binding protein (ABP1) is an important receptor for the plant hormone auxin that is involved with many growth and developmental responses in plants. The maize ABP1 gene has been expressed in insect cells, purified and crystallized. Type II crystals are monoclinic, with two glycosylated homodimers in the asymmetric unit, and diffract to 1.9 Å using synchrotron radiation.

1. Introduction

All aspects of plant growth and development are mediated by phytohormones and yet there is still little known about how these are perceived or of the signalling pathways they excite. As for other hormones, it is anticipated that specificity to phytohormones is conferred by high-affinity binding sites on receptor proteins. Few candidate receptors for phytohormones have been described, the exceptions being for ethylene (Ecker, 1995; Bleecker *et al.*, 1998), cytokinins (Plakidou-Dymock *et al.*, 1998) and auxin.

A great deal of work has gone into the characterization of the auxin-binding protein known as ABP1. Initially purified from maize (Löbler & Klämbt, 1985*a*,*b*), the structure, function and cell biology of ABP1 have been explored (Venis & Napier, 1995; Napier, 1997; Jones *et al.*, 1998) and an efficient expression system established using recombinant baculovirus (Macdonald *et al.*, 1994). However, until recently our knowledge of the structure of the protein has been limited to analysis of circular dichroism measurements (Shimomura *et al.*, 1986) and predictions of secondary structure (Inohara *et al.*, 1989), both of which suggested little α-helix and abundant β-sheet and β-turn. There has also been an awareness of a number of epitopes, presumed to lie on the surface of the native protein (Napier & Venis, 1992; Leblanc *et al.*, 1999), and of a conformational change induced by ligand binding (Shimomura *et al.*, 1986; Napier & Venis, 1990). Part of the sequence has been identified as the auxin-binding site (Venis *et al.*, 1992; Brown & Jones, 1994). More recently, searches using two sequence motifs [$G(X)_5HXH(X)_{11}G$ and $G(X)_5P(X)_4H(X)_3N$, where X is any amino-acid residue] have identified ABP1 as a member of the cupin superfamily (Gane *et al.*, 1998). The cupin superfamily includes germin, the structure of which has been solved recently (Woo *et al.*, 2000). Germin has little sequence similarity with ABP1, but the germin structure would suggest that ABP1 has a metal-binding histidine cluster located towards the end of a β-jellyroll barrel which would form the putative auxin-binding site.

In maize (*Zea mays* L.), the *ABP1* gene codes for a polypeptide of 201 residues, including a 38-residue signal peptide which is cleaved on entry into the endoplasmic reticulum. There is a single N-glycosylation site that carries an oligomannose glycan group (Henderson *et al.*, 1997). Expression in baculovirus-infected insect cells yields ABP1 that is glycosylated and that has auxin-binding kinetics indistinguishable from those of protein purified from maize (Macdonald *et al.*, 1994). We have used this expression system as a source of ABP1 for large-scale purification and crystallization. Under native conditions ABP1 is a homodimer (Löbler & Klämbt, 1985*a*).

2. Materials and methods

2.1. Expression and purification of ABP1

The *ABP1* gene codes for a protein with a C-terminal KDEL retention sequence which promotes its accumulation in the endoplasmic reticulum in plants (Napier, 1997) and baculovirus-infected insect cells (Macdonald *et al.*, 1994). In order to facilitate purification, this motif was mutated to KEQL, allowing a high percentage of ABP1 to be secreted to the culture medium (Henderson *et al.*, 1996). High-titre recombinant baculovirus stocks were prepared using standard protocols (King & Possee, 1992). *Trichoplusia ni* cells were cultured in Insect Xpress medium (Bio Whittaker, Wokingham, UK) in suspensions maintained at 80 rev min^{-1} and 291 K in an orbital shaker. Cells were infected at a high multiplicity of infection (Henderson *et al.*, 1997) at a density of 1×10^6 cells ml^{-1}. The medium was harvested at either 3 or 4 d after infection, cells were removed by centrifugation at 2000*g* and

Table 1
Summary of the crystallization conditions and data collected from type I, II and III crystals of auxin-binding protein ABP1.

For the measures of completeness, R_{merge} and average (I/σ) two values are given: the first is for the whole resolution range and the second, in parentheses, is for the highest resolution shell.

	Type I	Type II	Type III
Crystallization reservoir	16% PEG 8K, 19% MPD pH 8.5 (0.1 *M* Tris)	23% PEG 4K, 0.1 *M* NH_4OAc pH 5.5 (0.1 *M* acetate)	23% PEG 4K, 0.1 *M* NH_4OAc pH 5.5 (0.1 *M* acetate)
Cryoprotectant	26% PEG 4K, 12% 2-propanol, 8% MPD pH 6.5 (0.1 *M* cacodyl)	23% PEG 4K, 0.1 *M* NH_4OAc, 12% 2-propanol, 8% MPD pH 7.5 (0.1 *M* HEPES)	23% PEG 4K, 0.1 *M* NH_4OAc, 12% 2-propanol, 8% MPD pH 7.5 (0.1 *M* HEPES)
Space group	$P2_12_12_1$	$P2_1$	$P2_12_12$
Unit-cell parameters (Å,°)	a = 44.0, b = 87.9, c = 97.4	a = 62.4, b = 82.3, c = 69.8, β = 94.2	a = 45.4, b = 174.1, c = 43.9
Monomers per asymmetric unit	2	4	2
Extent of diffraction (Å)	3.1	1.9	2.75
Number of unique reflections	7297	54476	8018
Mosaicity (°)	1.30	0.47	1.0
Multiplicity	4	2	4
Completeness (%)	97.5 (86.5)	99.0 (99.0)	82.7 (83.0)
R_{merge}† (%)	15.5 (26.6)	4.0 (11.6)	7.1 (13.3)
Average (I/σ)	7.4 (3.4)	24.8 (6.1)	17.6 (9.0)

† $R_{merge}(I) = \sum|I_i - \langle I\rangle|/\sum I_i|$ where I_i is the intensity of the ith observation, $\langle I\rangle$ is the mean intensity of the reflection and the summation is taken over all data.

the cleared supernatant frozen in liquid nitrogen for storage at 193 K until use. After thawing, the medium was filtered through glass fibre (Whatman GF/B) and then a combined filter of 0.8 and 0.2 µm (Vacucap 90 PF, Gelman Sciences, Northampton, England) before concentration and buffer exchange using a Vivaflow 200 cell (with 10 kDa molecular-weight cutoff, Vivapore, Anachem, Luton, England). This concentrate was loaded onto a DEAE Fast Flow (Amersham Pharmacia Biotech, Milton Keynes, England) column (5.0 × 30 cm) in 20 m*M* Tris–HCl pH 7.2 containing 50 m*M* NaCl. After washing, ABP1 was eluted with 150 m*M* NaCl. The pH was adjusted to 5.5 with HCl and the sample was loaded onto a 5.0 × 20.0 cm phenylacetic acid–Sepharose column (Radermacher & Klämbt, 1993) equilibrated in 20 m*M* Mes–NaOH pH 5.5 with 150 m*M* NaCl, 1 m*M* $MgSO_4$ and 1 m*M* EDTA. The flow rate was chosen to give the sample between 1 and 2 h on the column. After a wash in the same buffer without salt, ABP1 was eluted in 20 m*M* Tris–HCl pH 9.1 and loaded directly onto a 1 ml HiTrap Q column (Pharmacia) equilibrated in 20 m*M* Tris–HCl pH 7.0. Using an NaCl gradient, ABP1 eluted at approximately 200 m*M* NaCl. For some preparations, the samples from the HiTrap Q column were concentrated in a Vivapore 10 cell and loaded onto an FPLC Superdex 75 10/30 column in 20 m*M* Tris–HCl pH 7.0 plus 150 m*M* NaCl. Fractions containing ABP1 were stored at 277 K with sodium azide (0.02%). Protein content was estimated from the absorbance at 280 nm. Yields were between 1 and 2 mg ABP1 per litre of medium. Purity was estimated from SDS–PAGE to be above 95%. The only significant contaminant was a breakdown product of ABP1 at 21 kDa, just smaller than the parent protein at 22 kDa (Napier & Venis, 1990).

2.2. Crystallization of ABP1

ABP1 was dialysed against 20 m*M* Tris buffer pH 7.0 with 1 m*M* $MgSO_4$ containing 2 m*M* sodium azide. The protein was concentrated to 8.5 mg ml^{-1} using a 10K cutoff membrane Centricon (Amicon). Crystals were grown at 291 K by the hanging-drop method, using the Hampton Screening Kits I and II which exploit the sparse-matrix protocol of Jancarik & Kim (1991). The hanging drops consisted of 2 µl of protein solution and 2 µl of reservoir solution.

2.3. Data collection and processing

X-ray diffraction data from a type II crystal were collected using the synchrotron at DESY, Hamburg, Germany, using a 300 mm imaging plate (MAR Research) on EMBL beamline X31. Data from type I and III crystals were obtained using a MacScience rotating-anode generator with double mirrors and a DIP 1030 image-plate system. Crystals were transferred to the appropriate cryoprotectant solutions, detailed in Table 1, before being cooled to 100 K in the nitrogen stream of an Oxford Cryosystems Cryostream. All data were collected using an oscillation range of 1°. The data were autoindexed and processed using *DENZO* and scaled using *SCALEPACK* (Otwinowski & Minor, 1997). All crystallographic calculations were made using the *CCP*4 program suite (Collaborative Computational Project, Number 4, 1994) unless otherwise stated.

3. Results and discussion

The functional ABP1 protein is a glycosylated homodimer with subunits of 163 amino acids and a molecular mass of approximately 22 kDa. Crystals of ABP1 grew in ten of the 50 drops of the initial screen (Hampton Crystallization Screen Kit I conditions 9, 10, 15, 17, 18, 22, 28, 40, 41 and 43). These ten trials all contained polyethylene glycol (PEG): either PEG 8000, PEG 4000 or PEG 1500. Three types of crystals were observed and characterized; two orthorhombic and one monoclinic (Table 1). Sharp-faceted type I crystals diffracting to 3.1 Å using a rotating-anode source were obtained by refining the initial crystallization conditions. The best type I crystals grew using a reservoir of 16% PEG 8000, 19% 2-methyl-2,4-pentanediol (MPD) and 0.1 *M* Tris buffer pH 8.5. A cryoprotectant solution comprising 26% PEG 4000, 12% 2-propanol, 8% MPD in 0.1 *M* cacodylate at pH 6.5 was found; this cryosolution with the addition of 0.1 *M* NH_4OAc was subsequently used successfully for cryo-cooling type II and III crystals. Type I crystals are orthorhombic, space group $P2_12_12_1$, with a = 44.0, b = 87.9, c = 97.4 Å and two monomers in the asymmetric unit, giving a V_M (Matthews, 1968) of 2.19 $Å^3\,Da^{-1}$. Type I crystals diffract rather poorly with high mosaicity.

Type II crystals grown using a reservoir of 23% PEG 4000 and 0.1 *M* ammonium acetate at pH 5.5 diffracted to 1.9 Å using a synchrotron source. They are oblique rectangular plates; they appeared after one week and grew after several weeks to a maximum size of 0.02 × 0.12 × 0.64 mm. Type II crystals are monoclinic, space group $P2_1$, with unit-cell parameters a = 62.4, b = 82.3, c = 69.8 Å, β = 94.2° and four monomers in the asymmetric unit, giving a V_M of 2.03 $Å^3\,Da^{-1}$.

Type III crystals grew as rectangular plates from the same crystallization conditions as type II crystals but are orthorhombic ($P2_12_12$), with unit-cell parameters a = 45.4, b = 174.1, c = 43.9 Å and two molecules in the asymmetric unit, giving a V_M of 2.03 $Å^3\,Da^{-1}$. Type III crystals diffracted to 2.75 Å using a rotating-anode

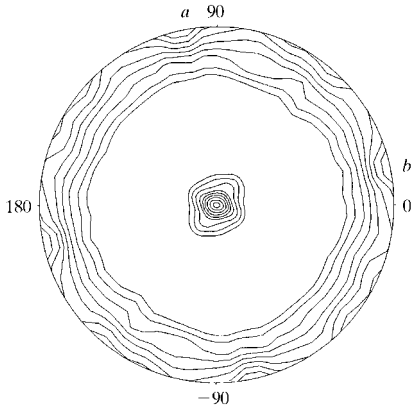

Figure 1
Self-rotation function $\kappa = 180^\circ$ section for type II ABP1 crystals reveals two non-crystallographic twofold axes at ω, φ angles of (8.1, 0°) and (98.1, 0°), respectively, consistent with two homodimers in the asymmetric unit. The calculation used an integration radius of 12 Å and a resolution range of 12–3 Å. The crystallographic twofold rotation axis is set to 100 and the contour level is 10.

source. The quality of the data measured from the three types of crystal is summarized in Table 1.

3.1. Non-crystallographic symmetry

Evidence for a non-crystallographic twofold axis in type I crystals comes from the presence of a peak at approximately 50% of the height of the crystallographic twofold axes at $\varphi = 90^\circ$ and $\omega = 45^\circ$ on the $\kappa = 180^\circ$ section. That is in the *bc* plane at 45° to both *b* and to *c*. There is evidence for a peak at a similar position in the type III crystals.

The self-rotation function for type II crystals reveals two non-crystallographic twofold axes ($\kappa = 180^\circ$) at ω, φ angles of (8.1,0°) and (98.1, 0°), respectively, consistent with two homodimers in the asymmetric unit (Fig. 1).

Multiple isomorphous replacement together with averaging will be used to solve the structure of ABP1. As the protein contains one free cysteine, mercurials will be screened initially.

We acknowledge use of the EMBL X31 beamline at the DORIS storage ring, DESY, Hamburg. We thank the Biotechnology and Biological Sciences Research Council of the UK for supporting this research and the Korean Ministry of Education for an award to EJW.

References

Bleecker, A. B., Esch, J. J., Hall, A. E., Rodriguez, F. I. & Binder, B. M. (1998). *Philos. Trans. R. Soc. London*, **353**, 1405–1412.
Brown, J. C. & Jones, A. M. (1994). *J. Biol. Chem.* **269**, 21136–21140.
Collaborative Computational Project, Number 4 (1994). *Acta Cryst.* D**50**, 760–763.
Ecker, J. R. (1995). *Science*, **268**, 667–675.
Gane, P. J., Dunwell, J. M. & Warwicker, J. (1998). *J. Mol. Evol.* **46**, 488–493.
Henderson, J., Bauly, J. M., Ashford, D. A., Oliver, S. C., Hawes, C. R., Lazarus, C. M., Venis, M. A. & Napier, R. M. (1997). *Planta*, **202**, 313–323.
Henderson, J., Macdonald, H., Lazarus, C. M., Napier, R. M. & Hawes, C. R. (1996). *Cell Biol. Int.* **20**, 413–422.
Inohara, N., Shimomura, S., Fukui, T. & Futai, M. (1989). *Proc. Natl Acad. Sci. USA*, **86**, 3564–3568.
Jancarik, J. & Kim, S.-H. (1991). *J. Appl. Cryst.* **24**, 409–411.
Jones, A. M., Im, K.-H., Savka, M. A., Wu, M. J., Dewitt, G., Shillito, R. & Binns, A. N. (1998). *Science*, **282**, 1114–1117.
King, L. A. & Possee, R. D. (1992). *The Baculovirus Expression System.* London: Chapman & Hall.
Leblanc, N., David, K., Grosclaude, J., Pradier, J. M., Barbier Brygoo, H., Labiau, S. & Perrot Rechenmann, C. (1999). *J. Biol. Chem.* **274**, 28314–28320.
Löbler, M., & Klämbt, D. (1985*a*). *J. Biol. Chem.* **260**, 9848–9853.
Löbler, M., & Klämbt, D. (1985*b*). *J. Biol. Chem.* **260**, 9854–9859.
Macdonald, H., Henderson, J., Napier, R. M., Venis, M. A., Hawes, C. & Lazarus, C. M. (1994). *Plant Physiol.* **105**, 1049–1057.
Matthews, B. W. (1968). *J. Mol. Biol.* **33**, 491–497.
Napier, R. M. (1997). *Trends Plant Sci.* **2**, 251–255.
Napier, R. M. & Venis, M. A. (1990). *Planta*, **182**, 313–318.
Napier, R. M. & Venis, M. A. (1992). *Biochem. J.* **284**, 841–845.
Otwinowski, Z. & Minor, W. (1997). *Methods Enzymol.* **276**, 307–326.
Plakidou-Dymock, S., Dymock, D. & Hooley, R. (1998). *Curr. Biol.* **8**, 315–324.
Radermacher, E. & Klämbt, D. (1993). *J. Plant Physiol.* **141**, 698–703.
Shimomura, S., Sotobayashi, T., Fukui, T. & Futai, M. (1986). *J. Biochem.* **99**, 1513–1524.
Venis, M. A. & Napier, R. M. (1995). *Crit. Rev. Plant Sci.* **14**, 27–47.
Venis, M. A., Napier, R. M., Barbier-Brygoo, H., Maurel, C., Perrot-Rechenmann, C. & Guern, J. (1992). *Proc. Natl Acad. Sci. USA*, **89**, 7208–7212.
Woo, E.-J., Dunwell, J. M., Goodenough, P. W. & Pickersgill, R. W. (2000). In the press.